Journal of Catalysis **183,** 53–62 (1999)
Article ID jcat.1998.2354, available online at http://www.idealibrary.com on IDEAL®

Characterization of La_2O_3/SiO_2 Mixed Oxide Catalyst Supports

H. Vidal,[1] S. Bernal, R. T. Baker, D. Finol, J. A. Pérez Omil, J. M. Pintado, and J. M. Rodríguez-Izquierdo

Departamento de Ciencia de los Materiales e Ingeniería Metalúrgica y Química Inorgánica, Facultad de Ciencias, Universidad de Cádiz, Apartado 40, Puerto Real, 11510 Cádiz, Spain

Received July 13, 1998; revised October 22, 1998; accepted November 10, 1998

Thermal analysis, energy dispersive spectroscopy, X-ray diffraction, high-resolution electron microscopy, X-ray photoelectron spectroscopy, and CO_2 adsorption have been applied to study a series of La_2O_3/SiO_2 samples with lanthana loadings ranging from 1.6 to 75 wt%. The results are interpreted on the basis of a lanthana–silica interaction model which assumes that patches of an amorphous La–Si–O phase, embedded in the silica matrix, modify the support surface in a progressive way, leading to a full coverage for 37.5% La_2O_3. This mixed silicate is soluble in acid media and its properties can be satisfactorily explained considering a structure which has a short-range order resembling that of crystalline $La_2Si_2O_7$. This behaviour differs from that described in the La_2O_3/Al_2O_3 system, more extensively studied in the literature, and from previous studies on La_2O_3/SiO_2 in which the formation of La_2O_3 particles on the silica surface was proposed. This contribution serves as a basis for understanding the additional promoting effect of lanthana in catalysts consisting of metals dispersed on modified silica supports.

Key Words: **La_2O_3/SiO_2 system; surface modification; lanthana–support interaction; La_2O_3/Al_2O_3 model.**

1. INTRODUCTION

Lanthana dispersed on conventional supports (Al_2O_3, SiO_2) may have, in itself, interesting applications in catalysis (1, 2). However, what is particularly significant is the fact that the characterization of this binary system may be crucial to understanding the role of lanthana as promoter when noble metals are deposited on the La_2O_3/support system (3, 4). For instance, the application of La_2O_3 either as a support (5, 6) or as a promoter in M/SiO_2 (M = Ni, Rh) (7) is receiving growing interest. These catalysts exhibit good performance in carbon dioxide reforming of methane to synthesis gas.

In spite of the parallelism discussed in the literature (8, 9), the analogies between La_2O_3/SiO_2 and La_2O_3/Al_2O_3 presented do not imply identical behaviours. In fact, a recent paper (10) outlined how M/La_2O_3–SiO_2 catalysts show clear advantages over M/La_2O_3–Al_2O_3 catalysts in certain cases. For example, the alumina may more easily favour the loss of the active metal phase through its incorporation into the support, as well as undesirable reactions due to the nature and reactivity of its surface acid groups, giving rise to catalysts which are more sensitive to deactivation. Thus, silica may be considered an interesting alternative to alumina. According to several authors (10, 11), the main disadvantages of silica are its loss of surface area under extreme reaction conditions as well as its very poor ability to interact with certain metals, which facilitates the sintering of the metal particles dispersed on its surface.

Much work has already been done on the study of lanthana-modified aluminas (12–23), whereas for the silica-based system the information available is much more scarce (24, 25). To our knowledge there is no work so far in the literature whose main focus is the characterization of La_2O_3/SiO_2 supports, as there is for La_2O_3/Al_2O_3. Additionally, most of the existing publications about La_2O_3-supported systems underline the promotion effects without analyzing in depth the nature of the promoting phase. Moreover, the few that do present such analysis usually refer to lanthana as though it were present as particles of crystalline La_2O_3 (14, 20, 26–29).

Nevertheless, recent studies show an evolution of these ideas by indicating that a distinction should indeed be established between alumina and silica when they are used as supports of rare earth oxides (10, 30, 31). In fact, several authors have found different properties for LnO_x/Al_2O_3 and LnO_x/SiO_2 systems that they correlate with differences in the interaction of the lanthanide with the support: whereas it seems that the lanthanide oxide is highly dispersed on alumina, most likely in the form of an amorphous phase, formation of a new mixed surface phase on silica has been described (30, 31). Furthermore, very recently Sellmer *et al.* (32) suggested that formation of a silicate could be at the root of the promotion effect observed in methanol synthesis over silica-supported Pd catalysts doped with additives such as Li, Ca, and La. In this paper we present data that are in line with these observations and that show clear differences between the modifications induced by lanthana

[1] To whom correspondence should be addressed. Fax: 34-956-834924. E-mail: hilario.vidal@uca.es.

0021-9517/99 $30.00

on silica and lanthana on alumina, suggesting that the parallelism with which both supported systems are still often considered might best be revised (20, 26, 33).

In (2) we reported on the properties of binary La_2O_3/support systems for CO hydrogenation, CO oxidation, and oxidative coupling of methane. Later we published some data obtained through the characterization of some La_2O_3/SiO_2 samples (34, 35). In this work, taking into account the above considerations, we move more deeply into the study of the silica-supported lanthana system. By using a wide number of complementary techniques in a way that has not been done before, we propose a structural model which explains satisfactorily the chemical behaviour observed. On the basis of this model, a comparison with La_2O_3/Al_2O_3, used as reference, is made.

2. EXPERIMENTAL DETAILS

In the present work, the support employed was SiO_2 Cabosil M-5 with a surface of 187 m^2/g after heating in air at 1173 K for 4 h. $La(NO_3)_3 \cdot 6H_2O$ from Fluka was used as the precursor for the supported lanthana. The lanthanum nitrate/silica samples were prepared by a one-step incipient wetness impregnation. Controlled amounts of the aqueous nitrate solutions were added to the silica in each case to obtain the final supported oxide phase with the desired La_2O_3 loading, which ranged from 1.6 to 75 wt% (expressed per gram of support). After the impregnation, the samples were dried in an oven at 363 K for 24 h. The final La_2O_3/SiO_2 samples were obtained by *in situ* calcination of the precursors in air at 873 K for 4 h before each experiment.

The specific surface areas of the above calcined samples, as determined by volumetric adsorption of N_2 at 77 K, have already been reported in (34) and range from 187 $m^2\ g^{-1}$ for pure silica to 157 $m^2\ g^{-1}$ silica for the highest lanthana loading. In this paper, surface area data for some of the samples measured using the same technique but after different calcination treatments are also presented.

To investigate the La_2O_3/SiO_2 system, five main characterization techniques have been applied: thermogravimetric analysis (TGA), X-ray diffraction (XRD), X-ray photoelectron spectroscopy (XPS), high-resolution electron microscopy (HREM), and carbon dioxide chemisorption. For the latter, temperature-programmed desorption (TPD) and FTIR spectroscopy after treatment with CO_2 as well as volumetric adsorption measurements have been used as complementary methods for analyzing the nature of CO_2 chemisorption. Also we have analyzed the aging in air of the samples by using TPD with mass spectrometry (MS) analysis (TPD-MS). For comparison purposes, we also include some results obtained for a La_2O_3/Al_2O_3 sample, with 20% lanthana loading, prepared in a similar way from 105 $m^2\ g^{-1}$ γ-Al_2O_3.

TGA analysis of the precursors was carried out with a Mettler HE thermobalance and MS with a VG Spectralab SX200 mass spectrometer. In the study of the interaction with carbon dioxide, prior to the TPD experiments, the samples were treated with flowing CO_2 at 60 $cm^3\ min^{-1}$, for 20 min. Then the gas flow was switched from CO_2 to helium for 60 min and the temperature was increased at a heating rate of 10 K min^{-1}.

The volumetric adsorption experiments were performed at 295 K in a conventional high-vacuum system, equipped with a MKS pressure transducer model BHS-1000. A conventional IR quartz cell was used to carry out the treatment on self-supported wafers of the samples. The cell allowed pretreatment in a flow of air, the evacuation under high vacuum, and further treatments with CO_2 at 1 atm pressure. The spectra were recorded on a Mattson 5020 FTIR instrument.

X-ray diffraction patterns of the samples calcined in air were recorded in a Siemens D-500 powder diffractometer operating with a Mo anode ($\lambda = 0.071$ nm).

XPS data discussed in the present work were obtained using a Leybold Heraeus LHS-10 electron spectrometer working with an Al anode (1486.6 eV) operating at 12 kV and 20 mA. HREM images were obtained in a JEOL 2000 EX microscope, with a top entry specimen holder and an ion pump, and with a structural resolution of 2.1 nm.

Microanalysis studies have also been performed with an EDS (energy dispersive spectroscopy) system coupled to a 820 JEOL scanning electron microscope. The instrument uses a 20-kV electron beam and is equiped with a LINK AN-10000 Si(Li) detector with Be window. With this technique 1 μm^2 areas of the material can be analyzed.

Finally, for the development of the structural model we have used the RHODIUS program developed in our laboratory (36, 37). Graphic representations of the supercell structural model built with this computer program were generated using an Indy 4400SC Silicon Graphics Workstation.

3. RESULTS AND DISCUSSION

3.1. Thermogravimetric Analysis

TGA diagrams corresponding to decomposition in static air of pure lanthanum nitrate and the lanthana-loaded samples (before calcination) were registered (results not shown). Three main observations were made from these experiments. First, experimental weight losses were consistent with La being present as $La(NO_3)_3 \cdot 6H_2O$. Second, decomposition of the La_2O_3/SiO_2 samples took place following a trend different from that for the pure nitrate. While for the latter, three clear features were observed in the TGA diagram, fitting well with water loss, formation of $LaONO_3$ and final sesquioxide formation, in the case of

the silica-supported samples only two regions of weight loss were detected: a first one, below 473 K, which must correspond with dehydration of the sample, and a second one, between 473 and 873 K, which can be correlated with the conversion of the nitrate into the final oxide. Finally, decomposition of the silica-supported lanthana samples took place at much lower temperatures than that of the pure nitrate, being complete at about 100 K below that of the unsupported sample, at around 873 K. For this reason this temperature was selected for the preparation of the La_2O_3/SiO_2 samples.

The last two observations can be considered a first indication of interaction between the lanthanum-containing phase and the support in the La_2O_3/SiO_2 mixed oxides.

3.2. Textural Study

Figure 1 represents how the lanthana loading affects the specific surface area (calculated per gram of silica) of the promoted samples. As lanthana loading increases a moderate decrease in surface area is seen initially. However, surface area seems to reach an approximately constant value at La_2O_3 loadings of 37.5% and above.

It is generally acknowledged that La_2O_3 plays an important role in the textural stabilization of alumina supports (17–19, 38–43). Therefore, an additional aim of this work was to determine whether La_2O_3 addition to silica enhanced the thermal stability of the support surface in a way similar to that commonly reported for La_2O_3/Al_2O_3.

In this sense, Fig. 2 shows that La_2O_3 slightly promotes the sintering of the silica particles. We think that it is the result of the easier aglomeration of the silica particles due to the modification induced by the presence of lanthana. The reaction between La_2O_3 and SiO_2, to be further discussed, will help us to understand why particles aglomerate more easily than in pure silica.

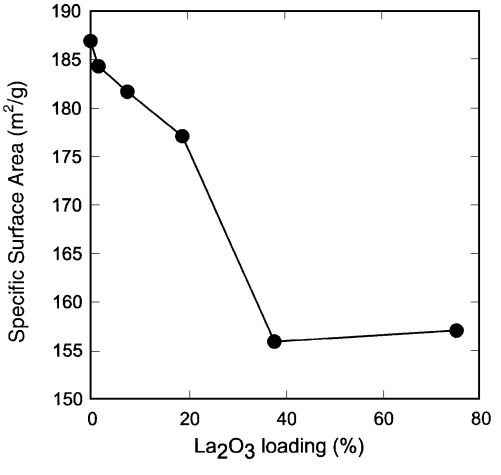

FIG. 1. Specific surface area referred to gram of silica for the La_2O_3/SiO_2 samples as function of lanthana loading.

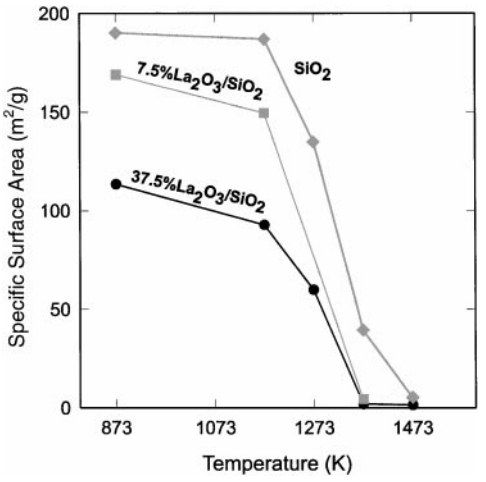

FIG. 2. Evolution with temperature of the specific surface area of the samples (treatment in air for 4 h at temperatures below 1273 K and during 24 h at 1273 K and above).

3.3. X-Ray Diffraction

The first step in the structural characterization of the La_2O_3/SiO_2 system was taken by employing XRD. Figure 3 shows the diffraction diagrams obtained for each of the mixed oxides. The diffraction pattern obtained for the 1.6%

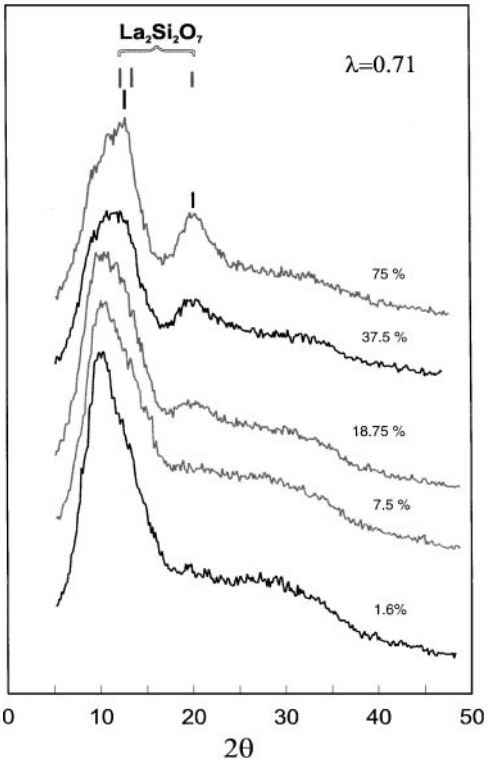

FIG. 3. X-ray diffraction patterns corresponding to the La_2O_3/SiO_2 samples obtained by heating their respective precursors in air at 873 K for 4 h. The loading for each sample is indicated.

La_2O_3/SiO_2 sample was very similar to that for pure SiO_2 (not shown). As the La_2O_3 loading increases, we observe that two broad peaks begin to grow in intensity. The broadness of these peaks is characteristic of a phase with low crystallinity, and their positions, around 2θ values of 13° and 21°, are not typical of any hydrated or carbonated phases of lanthana. However, they are in agreement with the position of peaks characteristic of a lanthanum disilicate phase, $La_2Si_2O_7$, according to JCPDS files [No. 21-1014].

If the samples are calcined above 1200 K we observe that the broad peaks transform into well-defined peaks at the positions expected for a $La_2Si_2O_7$. In conclusion, XRD shows indications of the incipient formation of a lanthanum disilicate phase.

3.4. High-Resolution Electron Microscopy

To study the microstructure of the samples HREM was employed. The La_2O_3/SiO_2 samples studied in the microscope were those with lanthana loadings of 7.5, 27, and 75%. The micrographs shown in Figs. 4 and 5 illustrate the general appearance of these samples. As a reference, a 20% La_2O_3/Al_2O_3 sample was also studied by HREM and a representative image obtained for this sample is also included in Fig. 5.

For the La_2O_3/SiO_2 sample with low loading (7.5%) we observe homogeneously dispersed particles with an average size of 4 nm (Fig. 4). Since the number of these particles increases with La_2O_3 loading we associate the particles with the lanthanum-containing phase. When we analyze samples of higher La_2O_3 loading, the particles, again homogeneously distributed, have similar appearance but are slightly larger (6–10 nm) (Fig. 5a). Thus the fraction of clean silica surface is much lower.

If we focus our attention on the particles viewed in profile, we note that they have an amorphous nature and that they seem not only to be deposited but also embedded into the support (Fig. 4). This suggests that during the calcination, the lanthanum reacts with the silica to form a mixed lathanum silicate phase, in good agreement with the XRD results. This is shown schematically in Fig. 6.

For the highest loading we can see how the whole silica surface has been modified by the formation of a silicate coating (Fig. 5b).

3.5. Dissolution Tests of La_2O_3/SiO_2

Analysis of the existing literature concerning M/Ln_2O_3 and $M/Ln_2O_3/Al_2O_3$ systems shows that the model usually proposed to describe the interaction between M and $4f$ oxide is that of metal decoration with nanoparticles of the lanthanide oxide (8, 44–49). Previous studies performed in our laboratory (45) demonstrated that such an effect might occur through total or partial redissolution of the lanthanide oxide during metal deposition via the impregnation technique. In this way, the fraction of oxide redissolved could then coprecipitate along with the metal during the drying step following the impregnation. Results by other authors support this proposal quite well (29, 50, 51).

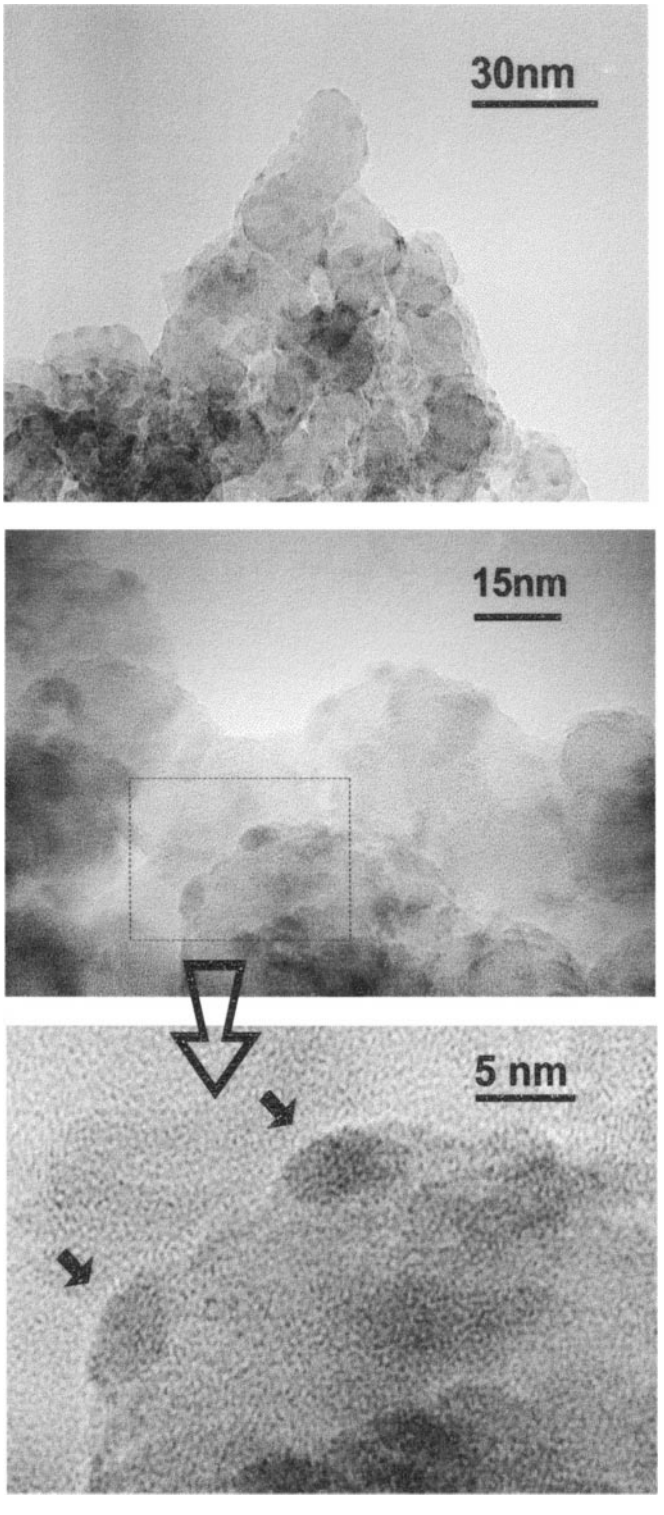

FIG. 4. HREM micrographs of the 7.5% La_2O_3/SiO_2 sample.

To see whether this effect also occurred with La_2O_3/SiO_2, we carried out some dissolution tests of the samples with

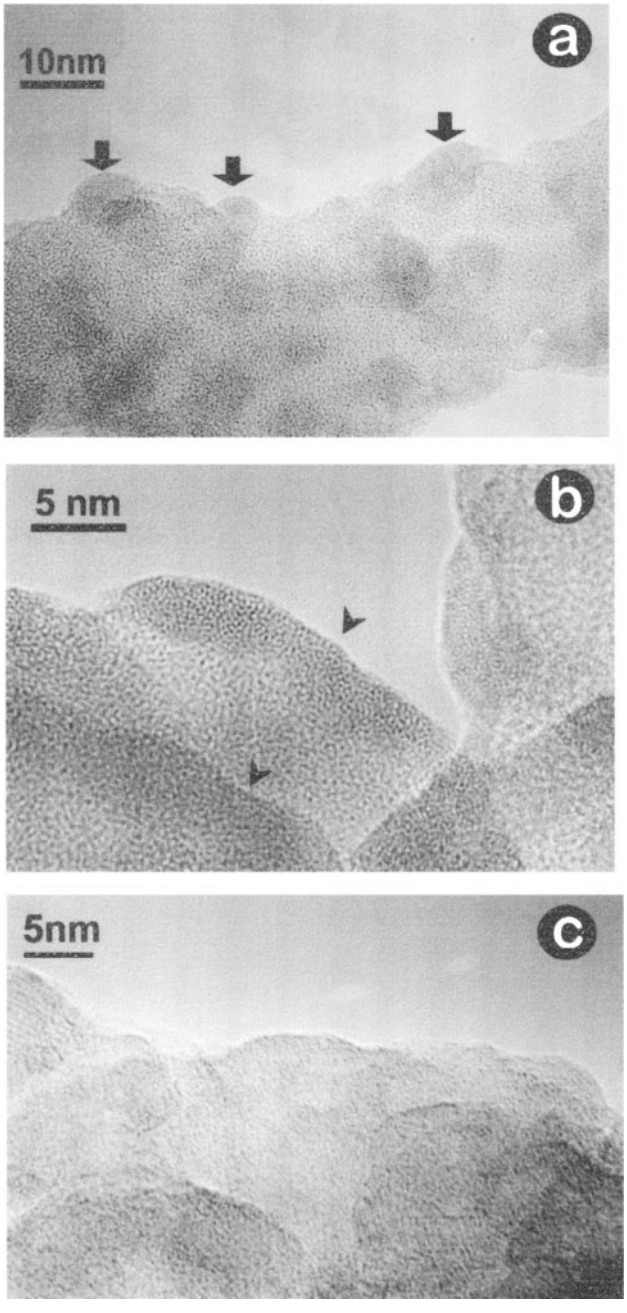

FIG. 5. HREM micrographs of (a) 27% La_2O_3/SiO_2, (b) 75% La_2O_3/SiO_2, and (c) 20% La_2O_3/Al_2O_3.

lanthana loadings of 18.75 and 75%, by treating them with aqueous solutions acidified with HNO_3 in order to simulate those used for metal impregnation. After being separated, washed, and dried, the resulting powders were analyzed by EDS to measure their lanthanum content.

Leaching with HNO_3 solution (pH = 1) and the analysis of the recovered powder and of the solid residue obtained from the solution also gave additional support to the hypothesis advanced above. EDS analysis showed that 100% of the lanthanum is leached from the La_2O_3/SiO_2 sample whilst the solid residue left after drying the extraction solution showed that both Si and La are present in a 1 : 1 ratio, as in the $La_2Si_2O_7$ phase.

If the sample is calcined at higher temperature, the amount of La extracted from the La_2O_3/SiO_2 sample decreases (Fig. 7). This suggests, as in previous work (4), that the crystallinity of the lanthanum silicate increased with increasing calcination temperature and that the leaching of the material by acid becomes more difficult. This is an important conclusion for the preparation of catalysts by impregnation of La_2O_3/SiO_2 supports with acidic solutions which contain metal precursors.

3.6. XPS Experiments

A 27% La_2O_3-loaded SiO_2 sample was studied by XPS. The results obtained are in agreement with the previous proposal. The La3*d*/Si2*s* ratio increases significantly with the calcination treatment, from a value of 0.18 for the fresh sample to 0.68 for the calcined one, suggesting that the calcination improves the level of dispersion of the lanthanum. Nevertheless, the apparent dispersion does not reach the level expected for a monolayer dispersion of La_2O_3. The theoretical value for a monolayer dispersion calculated according to models proposed in (33, 52) is 1.34. This difference can be understood assuming that particles of a silicate phase, in which a significant fraction of the lanthanum atoms are not present in the outer layer, are being formed. This result is in contrast with the behaviour of La_2O_3/Al_2O_3

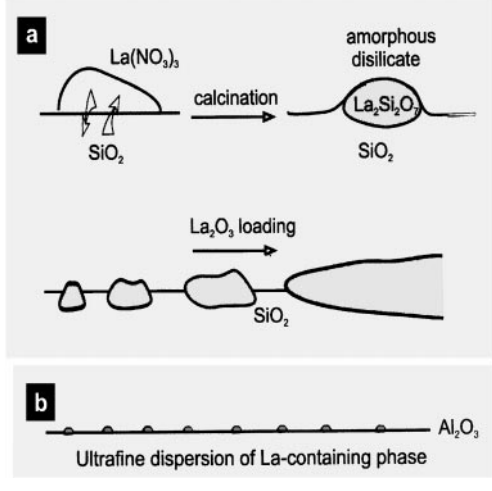

FIG. 6. Scheme illustrating the surface structural model proposed for (a) the La_2O_3/SiO_2 system and its comparison with (b) La_2O_3/Al_2O_3. The interaction between La_2O_3 and SiO_2 does not lead at first to the formation of a monolayer of the modified phase but instead reaction begins to take place with the SiO_2 before the entire silica surface has been modified. The phase resulting from this process is of a mixed and amorphous nature. For 37.5% lanthana loading almost the entire surface of silica is affected, and further addition of La_2O_3 implies only an increase in thickness of the modified crust.

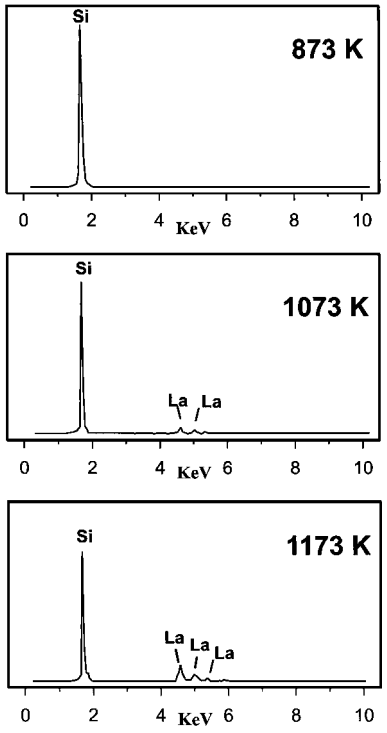

FIG. 7. EDS spectra obtained after disolution tests with HNO_3 solution (pH = 1) of the 18.75% La_2O_3/SiO_2 sample precalcined in air for 4 h at the indicated temperatures.

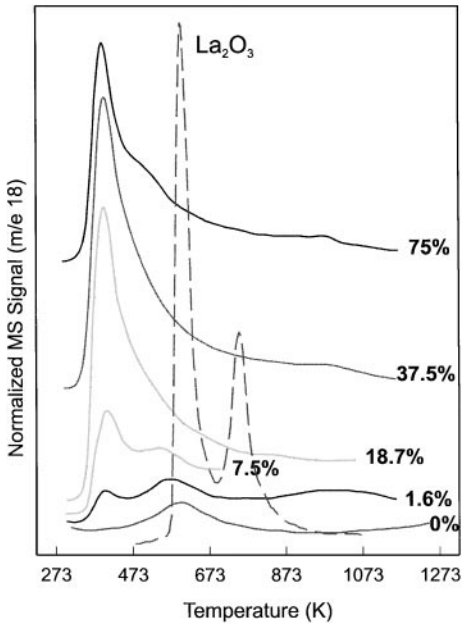

FIG. 8. H_2O traces corresponding to the TPD-MS experiments after aging in air of La_2O_3/SiO_2 samples (loading indicated) and pure La_2O_3.

systems (52) in which XPS data suggest an ultrafine dispersion of the La-containing phase on the alumina and for which we have never observed discrete particles on the surface of the alumina by HREM (Figure 5c), implying that the size of the particles, if they exist, must be below the detection limit of the electron microscope.

3.7. Aging in Air

It is well known that aging in air of La_2O_3 leads to a fast and complete transformation of the sesquioxide into partially carbonated $La(OH)_3$ (53). We have studied the chemistry of the hydration and carbonation of La_2O_3/SiO_2 samples, and found that it is quite different from that observed for La_2O_3 (53). This also suggests that lanthanum is not present as lanthanum oxide but rather forms a mixed phase with silica.

As an example we show the water evolution from lanthana compared to the water evolution from the mixed phase. In the mixed phases the process can be rationalized as a surface process, contrary to that for pure lanthana, in which it is a bulk process (Fig. 8) (53). Similar conclusions were derived from analysis of CO_2 evolution by TPD-MS (results not shown). While for aged La_2O_3 it is necessary to heat the sample above 1023 K to guarantee complete decarbonation and thus recover the original sesquioxide phase, in the case of the aged La_2O_3/SiO_2 samples the majority of CO_2 is evolved at around 400 K and no CO_2 is evolved above 873 K.

The weight gain resulting from hydration and carbonation of the La_2O_3/SiO_2 samples due to aging in air is completed in 1 h, and here again we observe that a plateau is reached at values of 37.5 wt% loading and above (Fig. 9). This effect can be interpreted as being associated with full coverage of the silica surface with the silicate phase. For higher loading the increase in lanthanum content would lead only to a thicker silicate phase.

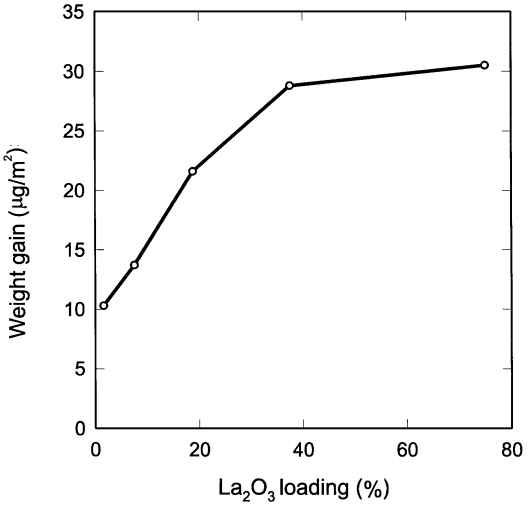

FIG. 9. Weight gain after aging in air at 295 K of the La_2O_3/SiO_2 system as a function of the lanthana loading, normalized to sample surface area.

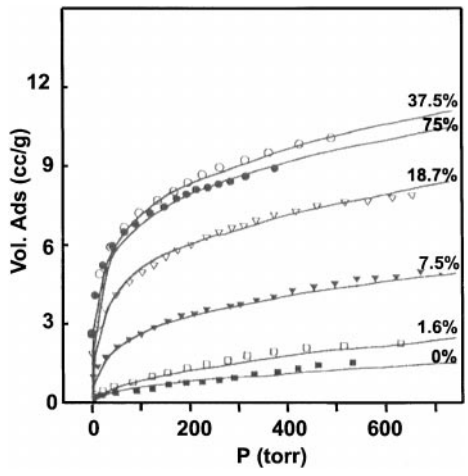

FIG. 10. CO_2 adsorption isotherms corresponding to the La_2O_3/SiO_2 samples (lanthana loading indicated).

3.8. Study of the Interaction with CO_2

An important aspect of the general characterization study performed on the La_2O_3/SiO_2 samples is CO_2 adsorption. A review of the literature demonstrates that the interaction with CO_2 can be used successfully to characterize LnO_x/Al_2O_3 systems (13–15, 21, 54, 55). In our case a detailed CO_2 adsorption study confirms same conclusions obtained in section 3.7.

The volumetric CO_2 adsorption isotherms of the samples were measured, and it was observed that the adsorption capacity increases with La_2O_3 loading (Fig. 10). Nevertheless, the volumes adsorbed for 37.5 and 75 wt% loading samples were very similar. Most of this adsorbed CO_2 (about 90%) was found to be weakly adsorbed since it was easily desorbed by evacuation at room temperature.

In Table 1 we observe a good agreement between the amount of CO_2 strongly (irreversibly) adsorbed estimated from the adsorption isotherms and that desorbed in the quantitative TPD experiments. The weakly adsorbed fraction is the most significant (about 10 times larger than for irreversible adsorption) and can only be determined from the isotherms. Nevertheless, the TPD experiments (Fig. 11) give useful information about the interaction between CO_2 and the surface and even allow us to propose a structure for the sample.

TABLE 1

Amounts of CO_2 (molec nm^{-2}) Determined by Integration of the TPD-MS Traces and from the Adsorption Isotherms on the La_2O_3/SiO_2 System

Loading (%)	Isotherm total	Isotherm irreversible	TPD-MS
75	2.8	0.26	0.27
37.5	2.5	0.26	0.26
18.75	1.4	0.09	0.11
7.5	0.8	0.05	0.07
1.6	0.34	0	0.023
0	0.22	0	0.003

The residual OH groups of the La_2O_3/SiO_2 samples have a very high thermal stability, similar to that of the OH groups for the pure silica. As CO_2 adsorption proceeds, a fraction of the OH groups decreases dramatically in thermal stability. The number of moles of CO_2 adsorbed determined from the isotherms is equal to the number of moles of OH evolved from the samples below 673 K calculated by integration of H_2O evolution peak in TPD. This led us to propose a model in which weakly adsorbed CO_2 molecules displace OH groups from their positions which coordinate to unsaturated La^{3+} at the surface of the silicate phase. In fact, some literature references (55, 56) have shown how the adsorption of CO_2, a molecule traditionally employed to detect basic sites, can also be successfully used to investigate the presence of weak Lewis acid sites on support surfaces.

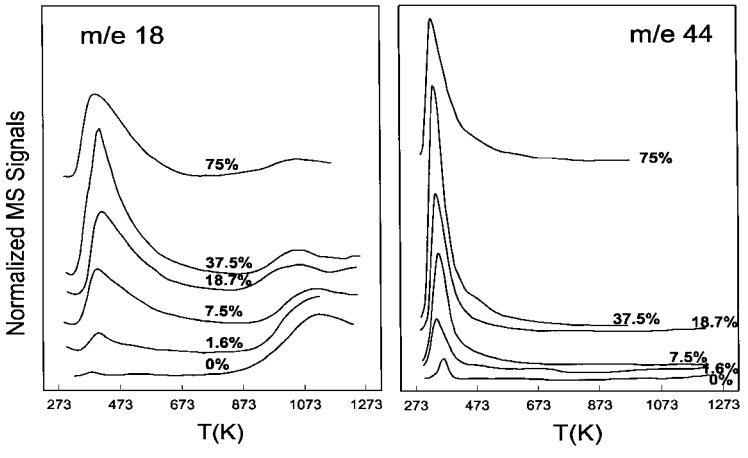

FIG. 11. CO_2 and H_2O traces corresponding to the TPD-MS experiments after treatment with CO_2 of the La_2O_3/SiO_2 samples (lanthana loading indicated).

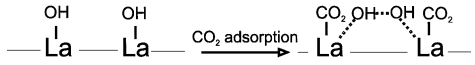

FIG. 12. Model proposed for the CO_2 interaction with the La_2O_3/SiO_2 samples: The CO_2 adsorption allows the OH groups to shift from their position and to approach each other, leading to an incipient interaction which favours their subsequent desorption at lower temperatures.

When the above OH groups are displaced from their positions, they can approach more easily their neighbouring OH groups, thus explaining the release of water at lower temperature (Fig. 12). The effect of such OH displacement is irreversible, because if we desorb the weakly adsorbed CO_2, the OH groups do not return to their starting positions. This is noted because in the TPD experiments the weakly adsorbed CO_2 desorbs at ambient temperature before the start of the experiment and, even so, the H_2O still desorbs at the same low temperature.

The FTIR results (Fig. 13) show that the weak CO_2 adsorption can be assigned to a band peaking at a frequency very similar to that of gaseous CO_2 (2340 cm^{-1}), which can be eliminated by room temperature evacuation. The much smaller amount of strongly adsorbed CO_2 appears in forms which are characteristic of bicarbonate groups (13) (3727, 3711, 1661, and 1634 cm^{-1}).

We have used a model of the (100) plane of the crystalline pyrosilicate structure as an approach to understanding the behaviour of our system (57, 58). We assume that the short-range order of the amorphous disilicate resembles the long-range order of the crystalline phase, allowing a rough understanding of its behaviour.

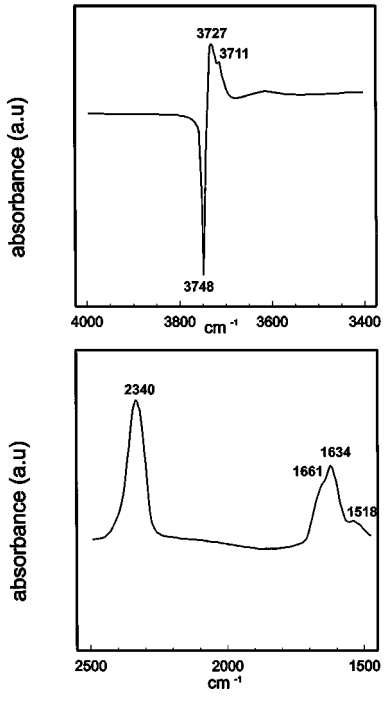

FIG. 13. Difference between the FTIR spectrum of 18.75% La_2O_3/SiO_2 treated with CO_2 and the spectrum of the untreated sample. Absorbance in arbitrary units versus wavenumber.

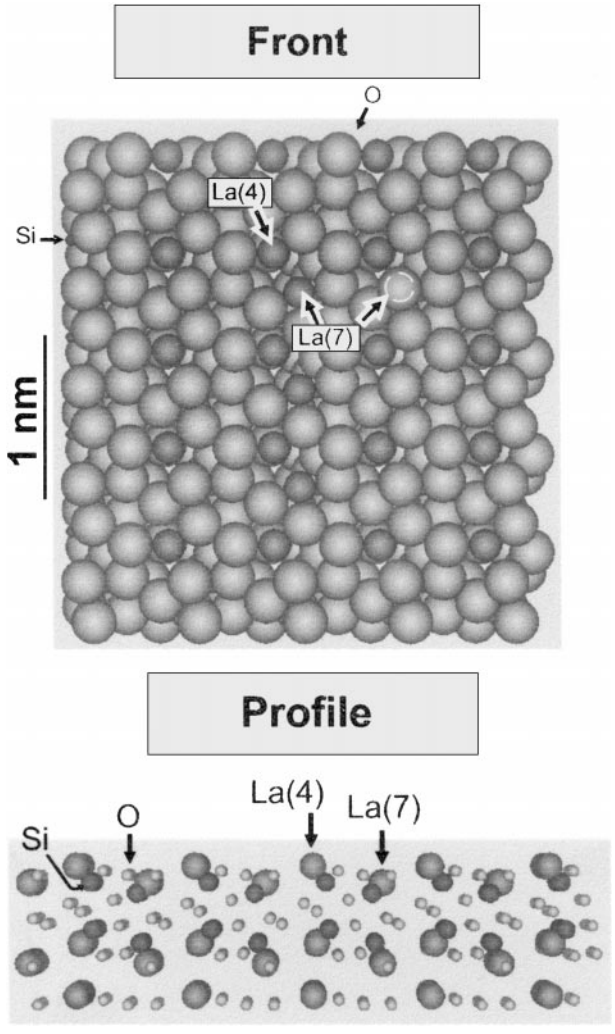

FIG. 14. Frontal and profile projections of the (100) plane corresponding to the $La_2Si_2O_7$ structure constructed considering only short-range order. Coordination numbers of La are indicated in parentheses. Broken circle indicates position of La(7) atom masked by overlying O. Overlying Os have been removed to show positions of 3 La(7) atoms. Note that atomic radia have been changed in the profile view to allow easier visualization of the structure.

In this plane (Fig. 14) we observe highly unsaturated La cations with coordination number 4 and weakly unsaturated La with coordination number 7. The first would require shielding by OH or other groups. The concentration of La^{3+} with coordination number 4 in this model would be 2.4/nm^2, in acceptable agreement with the amount of CO_2/nm^2 adsorbed over the 37.5 and 75% loading samples (Table 1).

4. CONCLUSIONS

(1) The main objectives of our study have been a detailed characterization of the La_2O_3/SiO_2 system and the

determination of the mechanisms of La_2O_3–SiO_2 interaction in order to provide a good basis for a further investigation of the structure and the catalytic properties of La_2O_3/SiO_2-supported metal systems. As mentioned in the Introduction, it has been generally established that rare earth oxides play an important promoting role on silica by improving the dispersion of metals and modulating the selectivity in metal-catalyzed reactions. However, to our knowledge, it is also evident that a satisfactory explanation of these promoting effects has not yet been presented.

(2) Taking into account that the La_2O_3/Al_2O_3 system has been the subject of much attention (12–14, 16, 19–22) and that it shows analogies in some aspects of its behaviour with those exhibited by La_2O_3/SiO_2 (8, 9), we have used it as a reference.

(3) It has been confirmed that lanthana is not effective in stabilizing the silica surface area during high-temperature treatments in the way that it is known to stabilize Al_2O_3 (Fig. 2).

(4) Dispersed lanthana particles are not formed in the La_2O_3/SiO_2 system, contrary to what has been reported in several previous studies on La_2O_3/Al_2O_3. Instead, amorphous and embedded particles of a mixed silicate phase have been observed, even for low La_2O_3 loadings (see Fig. 4). This clearly contradicts what has been found very recently by Craciun and Dulamita (26), who reported that, after calcination of La_2O_3/SiO_2 catalysts, small La_2O_3 crystallites are formed on the silica surface. On the contrary, our results are in agreement with Shen *et al.* (30), who, studying Eu_2O_3 supported on silica by different techniques including microcalorimetry, XRD, and FTIR, did not observe formation of crystalline oxide particles over the support.

(5) The coverage of the mixed silicate increases with the La_2O_3 loading, in such a way that for the 37.5% lanthana loading, the silica surface is completely covered. The loading required for maximum coverage depends on the surface area of the SiO_2 used and hence will be different for different silicas. Therefore the value given is true only for the SiO_2 used in this study.

(6) The amorphous silicate phase is soluble in acid media, which might have significance for the preparation of M/La_2O_3–SiO_2 samples.

(7) On the basis of the crystalline $La_2Si_2O_7$ structure we propose a model which allows an interpretation of the chemical behaviour observed.

ACKNOWLEDGMENTS

This work received financial support from DGICYT, under Contracts PB94-1305 and PB95-1257, as well as from CICYT, under Contract MAT95-960931. We thank the Centralized Services of Science and Technology of the University of Cádiz for use of their facilities to obtain both the HREM images and the XRD diagrams.

REFERENCES

1. Bin-Yan, H., and Wan, L., *J. Less Common Met.* **112**, 343 (1985).
2. Castiglioni, J., Kieffer, R., Botana, F. J., Calvino, J. J., Rodríguez-Izquierdo, J. M., and Vidal, H., *J. Alloys Comp.* **180**, 295 (1992).
3. Imamura, K., and Misono, M., *Shokubai* **37**, 198 (1995).
4. Bernal, S., Blanco, G., Calvino, J. J., Cauqui, M. A., Rodríguez-Izquierdo, J. M., and Vidal, H., *J. Alloys Comp.* **250**, 461 (1997).
5. Zhang, Z., Verykios, X. E., McDonald, S. M., and Affrossman, S., *J. Phys. Chem.* **100**, 744 (1996).
6. Zhang, Z., and Verykios, X. E., *Catal. Lett.* **38**, 175 (1996).
7. Gronchi, P., Centola, P., and Del Rosso, R., *Appl. Catal. A* **152**, 83 (1997).
8. Rieck, J. S., and Bell, A. T., *J. Catal.* **99**, 278 (1986).
9. Underwood, R. P., and Bell, A. T., *J. Catal.* **111**, 325 (1988).
10. Deeba, M., Farrauto, R. J., and Lui, Y. K., *Appl. Catal. A* **124**, 339 (1995).
11. Lamber, R., Jaeger, N., and Schulz-Ekloff, G., *J. Catal.* **23**, 285 (1990).
12. Ledford, J. S., Houalla, M., Petrakis, L., and Hercules, D. M., *Stud. Surf. Sci. Catal.* **31**, 433 (1987).
13. Alvero, R., Bernal, A., Carrizosa, I., and Odriozola, J. A., *Inorg. Chim. Acta* **140**, 45 (1987).
14. Bettman, M., Chase, R. E., Otto, K., and Weber, W. H., *J. Catal.* **117**, 447 (1989).
15. Odriozola, J. A., Carrizosa, I., and Alvero, R., *Stud. Surf. Sci. Catal.* **48**, 713 (1989).
16. Ledford, J. S., Houalla, M., Proctor, A., Hercules, D. M., and Petrakis, L., *J. Phys. Chem.* **93**, 6770 (1989).
17. Johnson, M. F. L., *J. Catal.* **123**, 245 (1990).
18. Ozawa, M., Kimura, K., and Isogai, A., *J. Less Common Met.* **162**, 297 (1990).
19. Bèguin, B., Garbowski, E., and Primet, M., *Appl. Catal.* **75**, 119 (1991).
20. Subramanian, S., Chattha, M. S., and Peters, C. R., *J. Mol. Catal.* **69**, 834 (1991).
21. Haack, L. P., De Vries, J. E., Otto, K., and Chattha, M. S., *Appl. Catal. A* **82**, 199 (1992).
22. Cui, J. W., Massoth, F. E., and Topsoe, N. Y., *J. Catal.* **136**, 361 (1992).
23. Shen, J., Cortright, R. D., Chen, Y., and Dumesic, J. A., *J. Phys. Chem.* **98**, 8067 (1994).
24. Tan, Y., Dou, L., Lu, D., and Wu, D., *J. Catal.* **129**, 447 (1991).
25. Imamura, H., Sakata, Y., and Tsuchiya, S., *J. Alloys. Comp.* **193**, 62 (1993).
26. Craciun, R., and Dulamita, N., *Catal. Lett.* **46**, 229 (1997).
27. Haddad, G. J., Chen, B., and Goodwin, J. G., *J. Catal.* **160**, 43 (1996).
28. Muraki, H., Shinjoh, H., and Fujitani, Y., *Appl. Catal.* **22**, 325 (1986).
29. Borer, A. L., and Prins, R., *Stud. Surf. Sci. Catal.* **75**, 765 (1993).
30. Shen, S., Lochhead, M. J., Bray, K. L., Chen, Y., and Dumesic, J. A., *J. Phys. Chem.* **99**, 2384 (1995).
31. Zhang, X., Walters, A. B., and Vannice, M. A., *in* "Programme of the 11th International Congress on Catalysis," Po-208. 1996.
32. Sellmer, C., Prins, R., and Kruse, N., *Catal. Lett.* **47**, 83 (1997).
33. Fígoli, N. S., L'Argentiere, P. C., Arcoya, A., and Seoane, X. L., *J. Catal.* **155**, 95 (1995).
34. Bernal, S., Calvino, J. J., Rodríguez-Izquierdo, J. M., Vidal, H., Castiglioni, J., and Kieffer, R., *J. Rare Earths* **2**, 834 (1991).
35. Blanco, G., Calvino, J. J., Cauqui, M. A., Cifredo, G. A., Pérez-Omil, J. A., Rodríguez-Izquierdo, J. M., and Vidal, H., *J. Alloys. Comp.* **207/208**, 201 (1994).
36. Bernal, S., Botana, F. J., Calvino, J. J., Cifredo, G. A., Pérez-Omil, J. A., and Pintado, J. M., *Catal. Today* **23**, 219 (1995).
37. Bernal, S., Botana, F. J., Calvino, J. J., López-Cartes, C., Pérez-Omil, J. A., and Rodríguez-Izquierdo, J. M., *Ultramicroscopy* **72**, 135 (1998).
38. Arai, H., and Machida, M., *Appl. Catal. A* **138**, 161 (1996).
39. Schaper, H., Doesburg, E. B. M., and Van Reijen, L. L., *Appl. Catal.* **7**, 211 (1983).

40. Schaper, H., Amesz, D. J., Doesburg, E. B. M., and Van Reijen, L. L., *Appl. Catal.* **9**, 129 (1984).
41. Koryabkina, N. A., Shkrabina, R. A., Ushakov, V. A., Lausberg, M., Keptein, F., and Ismagilov, Z. R., *Kinet. Catal.* **38**, 112 (1997).
42. Zwinkels, M. F. M., Jaras, S. G., and Menon, P., *Catal. Rev. Sci. Eng.* **35**, 319 (1993).
43. Church, J. S., Cant, N. W., and Trimm, D. L., *Appl. Catal. A* **101**, 105 (1993).
44. Yu-Hua, D., De-An, C., and Khi-Rui, T., *Appl. Catal.* **35**, 77 (1987).
45. Kieffer, R., Kiennemann, A., Rodríguez, M., Bernal, S., and Rodríguez-Izquierdo, J. M., *Appl. Catal.* **42**, 77 (1988).
46. Underwood, R. P., and Bell, A. T., *Appl. Catal.* **21**, 157 (1986).
47. Underwood, R. P., and Bell, A. T., *Appl. Catal.* **34**, 289 (1987).
48. Gallaher, G. R., Goodwin, J. G., Jr., and Guczi, L., *Appl. Catal.* **73**, 1 (1991).
49. Gallaher, G., Goodwin, J. G., Jr., Huang, C., and Houalla, M., *J. Catal.* **127**, 719 (1991).
50. Dou, L., Tan, Y., and Lu, D., *Appl. Catal.* **66**, 235 (1990).
51. Tan, Y., Dou, L., Lu, D., and Wu, D., *J. Catal.* **129**, 447 (1991).
52. Kerkhof, F. P. J. M., and Moulijn, J. A., *J. Phys. Chem.* **83**, 1612 (1979).
53. Bernal, S., Botana, F. J., García, R., and Rodríguez-Izquierdo, J. M., *React. Solids* **4**, 23 (1987).
54. Alvero, R., Bernal, A., Carrizosa, I., Odriozola, J. A., and Trillo, J. M., *Appl. Catal.* **25**, 207 (1986).
55. Morterra, C., Magnacca, G., Filippi, G., and Giachello, A., *J. Catal.* **137**, 346 (1992).
56. Shen, J., Cortright, R. D., Chen, Y., and Dumesic, J. A., *J. Phys. Chem.* **98**, 8067 (1994).
57. Pearson, W. P., "Structure Reports," Vol. 35A, p. 484. International Union of Crystallography/Oosthoek, Scheltema & Holkema, Utrecht, 1970.
58. Smolin, B. Y. I., and Shepelev, Y. F., *Acta Crystallogr. Sect. B* **26**, 484 (1970).